

Supplementary information

Pomegranate Seed Polyphenol-based Nanosheets as an Efficient Inhibitor of Amyloid Fibril Assembly and Cytotoxicity of HEWL

Ali Akbar Meratan¹, Vahid Hassani¹, Atiyeh Mahdavi¹, Nasser Nikfarjam²

¹ Department of Biological Sciences, Institute for Advanced Studies in Basic Sciences (IASBS), Zanjan 45137-66731, Iran.

² Department of Chemistry, Institute for Advanced Studies in Basic Sciences (IASBS), Zanjan 45137-66731, Iran.

Figure S1. The obtained powders of polyphenolic fraction of Pomegranate seed (PFPS) corresponding to (A) bulk and (B) nano forms. (C) Aqueous solution (2.5 mg mL^{-1}) of bulk and nano forms of PFPS.

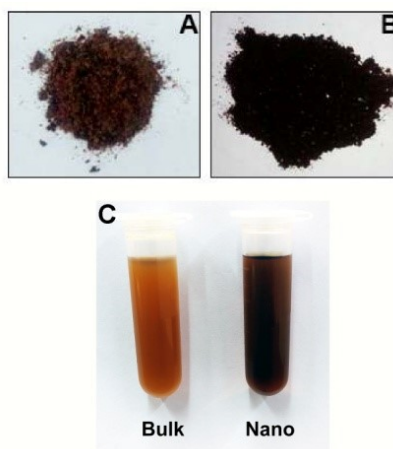


Figure S2. Fluorescence emission spectra of the bulk form of PFPS, excited at different wavelengths.

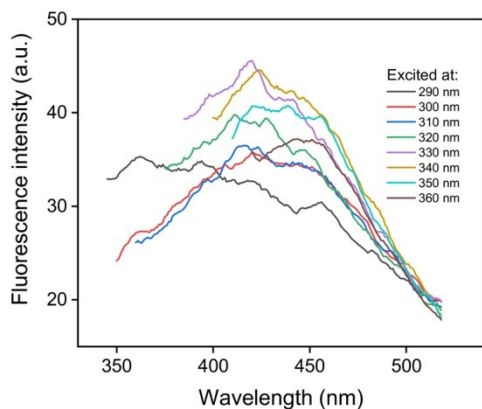


Figure S3. Fluorescence emission properties of (A) bulk and (B) nano forms of PFPS. Left-hand and right-hand y axes show fluorescence emission intensity and maximum emission wavelength of the bulk/nano forms of PFPS as a function of excited wavelength, respectively.

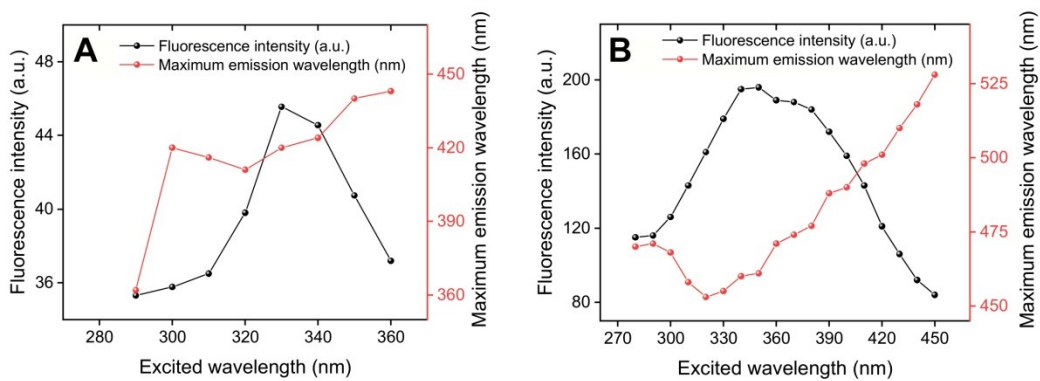


Figure S4. FT-IR spectra of the bulk and nano forms of PFPS.

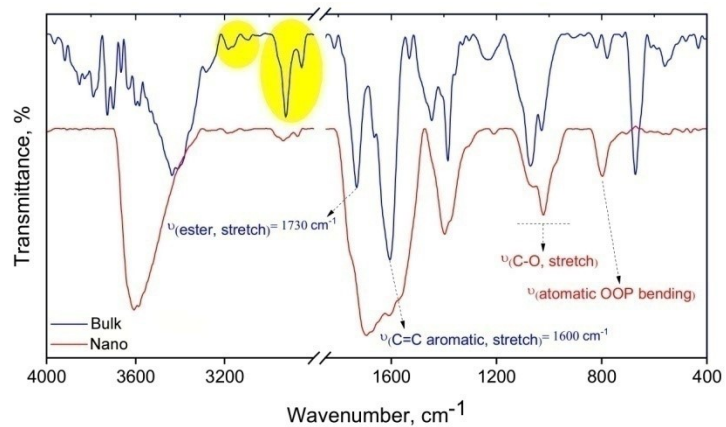


Figure S5. Surface zeta potential of PFPS nanosheets as a function of pH.

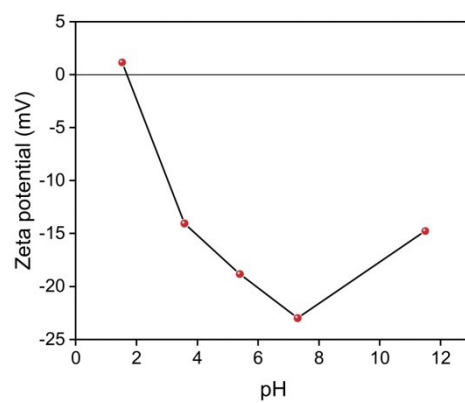


Figure S6. FE-SEM images of PFPS nanosheets. Due to the plenty of oxygen-based functional groups along with aromatic domains on the surface and sides of prepared nanoparticles, these structures are very susceptible to interact together, through hydrogen bonding and π - π stacking, and form large aggregates.

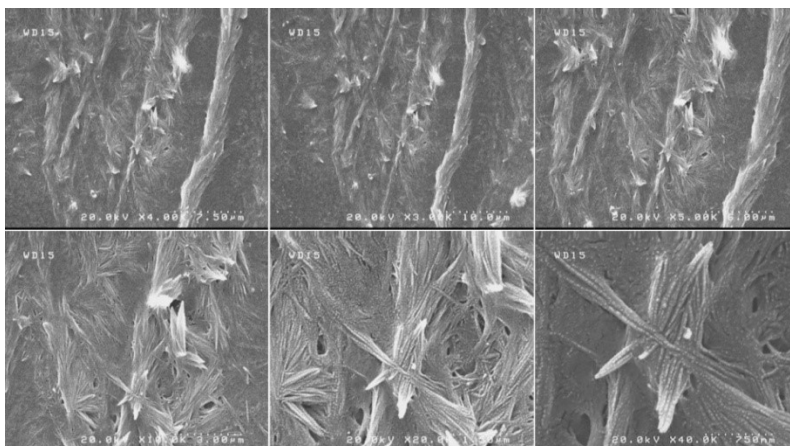


Figure S7. Congo red binding absorption spectra of HEWL in the absence and presence of various concentrations of (A) bulk or (B) nano forms of PFPS. (C) Quantification of Congo red binding.

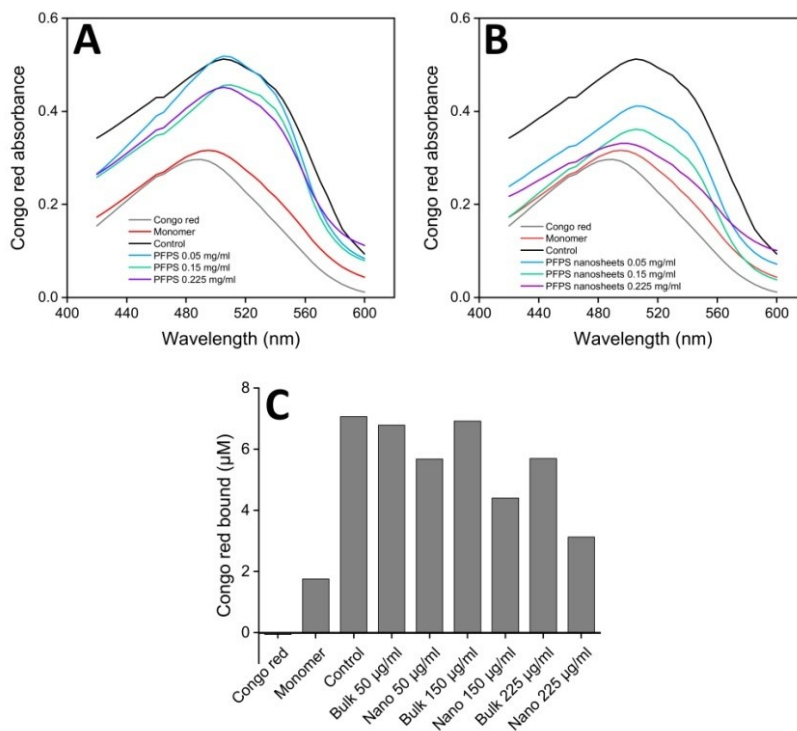


Figure S8. Dose-dependent toxicity of the bulk and nano forms of PFPS evaluated by MTT-based cell viability assay.

*p < 0.01, **p < 0.001, were significantly different from control cells.

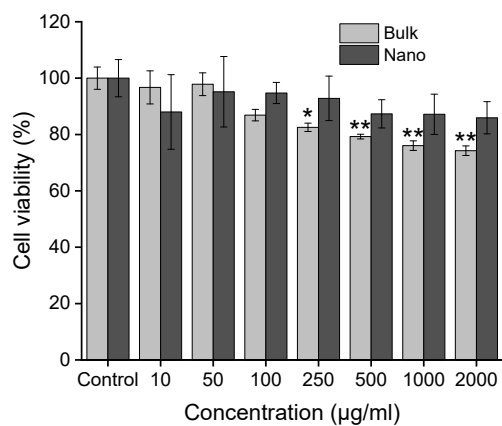


Figure S9. Dose-dependent toxicity of HEWL amyloid fibrils evaluated by MTT-based cell viability assay. *p < 0.01,

**p < 0.001, were significantly different from control cells.

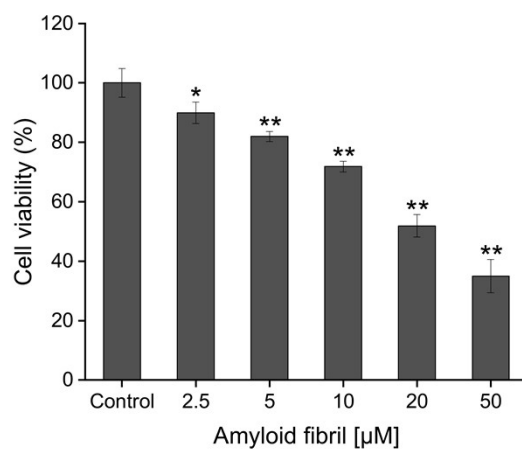


Figure S10. Dose-dependent hemolytic activity of the bulk and nano forms of PFPS. The percentage of hemolysis is calculated as percentage of the maximum observed upon treatment with Triton X-100 (1%). Low panels show optical microscopy images of samples incubated either alone (A) or with different concentrations of 50 (B), 150 (C), and 400 (D) $\mu\text{g mL}^{-1}$ bulk, or 50 (E), 150 (F), and 400 (G) $\mu\text{g mL}^{-1}$ nano forms of PFPS. (H) An enlarged view of (G). Arrows indicate the permeabilized cells.

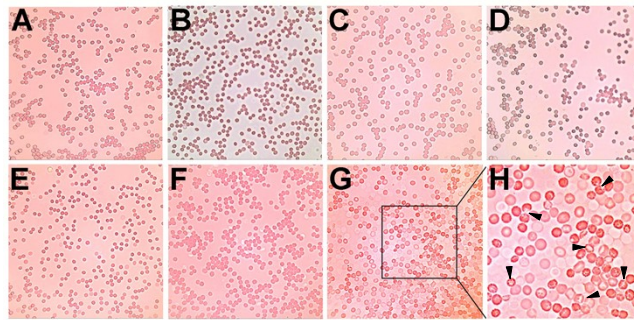
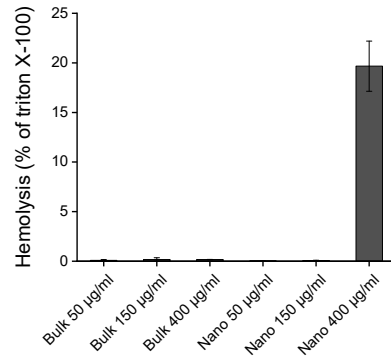


Figure S11. Dose-dependent hemolytic activity of HEWL amyloid fibrils. The percentage of hemolysis is calculated as percentage of the maximum observed upon treatment with Triton X-100 (1%). Inset shows erythrocyte aggregation induced by 50 μM HEWL amyloid fibril.

